Bioorganic & Medicinal Chemistry 16 (2008) 7371–7376

Contents lists available at ScienceDirect

Bioorganic & Medicinal Chemistry

journal homepage: www.elsevier.com/locate/bmc

Enhanced affinity of ketotifen towards tamarind-seed polysaccharide in comparison with hydroxyethylcellulose and hyaluronic acid: A nuclear magnetic resonance investigation

Gloria Uccello-Barretta [a,*], Samuele Nazzi [a], Federica Balzano [a], Giacomo Di Colo [b], Ylenia Zambito [b], Chiara Zaino [b], Marco Sansò [c], Eleonora Salvadori [c], Marco Benvenuti [c]

[a] Università di Pisa, Dipartimento di Chimica e Chimica Industriale, Via Risorgimento 35, I-56126 Pisa, Italy
[b] Università di Pisa, Dipartimento di Chimica Bioorganica e Biofarmaceutica, Via Bonanno 33, I-56126 Pisa, Italy
[c] Farmigea SpA, Via G.B. Oliva 8, I-56121 Pisa, Italy

ARTICLE INFO

Article history:
Received 4 February 2008
Revised 6 June 2008
Accepted 11 June 2008
Available online 14 June 2008

Keywords:
NMR
DOSY
Selective relaxation rates
Tamarind-seed polysaccharide
Ketotifen
Affinity

ABSTRACT

Nuclear magnetic resonance (NMR) spectroscopy demonstrated that, in aqueous solution, ketotifen fumarate bound more strongly to tamarind-seed polysaccharide (TSP) than to hydroxyethylcellulose or hyaluronic acid. Results were confirmed by dynamic dialysis technique.

1. Introduction

Polysaccharides are relatively complex carbohydrates. They provide good mechanical properties for applications as fibers, films, adhesives, rheology modifiers, hydrogels, emulsifiers and drug delivery agents. For instance, some polysaccharides have proven to enhance the contact between drug and human mucosa due to their high mucoadhesive properties. The growing interest in these last applications requires the development of methods for elucidating the interaction mechanism of small ligands with polysaccharides, among which equilibrium dialysis, ultrafiltration, size-exclusion chromatography, capillary electrophoresis, and fluorescence spectroscopy are widely employed. The disadvantages of some of these methods include the necessity for some kind of separation during the analysis, which can perturb the binding equilibrium, or the need for fluorescent probes or derivatization for labelling purposes. Nuclear magnetic resonance (NMR) spectroscopy is an attractive technique for studying ligand–macromolecule interactions because a single kind of analysis can yield a vast amount of structural information without destroying the sample. Although inherently insensitive relative to many other analytical techniques, nearly all molecules have NMR active nuclei, meaning that the technique is universal and analyte derivatization is unnecessary. Furthermore, analyzing intact mixture, without effecting a separation, simplifies and quickens the analysis. Among NMR methods[1] employed for investigating drug–macromolecule adducts the evaluation of so called 'affinity index',[2] as well as the determination of dipole–dipole cross-relaxation parameters[3] are particularly efficient in order to compare the strength of the interaction processes involving the same drug and different polymers, or the same macromolecule and different ligands. Evaluation of both parameters can be based on proton selective relaxation rates measurements, which are significantly sensitive to slowing down of drug molecular motion due to drug–macromolecule interaction. An alternative way to an efficient detection of drug–macromolecule interactions comes from diffusion ordered spectroscopy (DOSY) measurements of translational diffusion coefficients.[4]

In the present paper, we employed 'affinity index', cross-relaxation rates and diffusion coefficient determinations to investigate the interactions between ketotifen fumarate (KT), an H1-anthistamine/mast cell stabilizer (Fig. 1), and three different polysaccharides, namely, hydroxyethylcellulose (HEC), a water-soluble cellulose derivative, hyaluronic acid (HA), an anionic biocompatible, non-immunogenic and biodegradable glycosaminoglycan, and a galactoxyloglucan polysaccharide extracted from tamarind

* Corresponding author. Fax: +39 0502219260.
E-mail address: gub@dcci.unipi.it (G. Uccello-Barretta).

0968-0896/$ - see front matter © 2008 Elsevier Ltd. All rights reserved.
doi:10.1016/j.bmc.2008.06.020

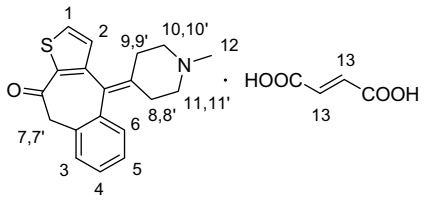

Figure 1. Ketotifen fumarate (KT).

seeds (TSP),[5] structure of which has been investigated by Gidley et al. in 1991.[5c] The above-mentioned polysaccharides are employed in medical formulations of ketotifen fumarate for ophthalmic use, to treat allergic conjunctivitis, or the itchy red eyes caused by allergies.

Polysaccharides, such as HEC, HA and TSP, may be expected to reside in the precorneal area for relatively prolonged periods, in virtue of their mucoadhesivity and/or viscosity, which slow down the clearance via the nasolacrimal drainage system. Hence, possible molecular KT–polysaccharide binding could prolong the residence of the drug in the precorneal area, thus improving the therapeutic efficacy of the formulation. In this view, comparing the ability of polymers to bind KT could correspond to making a comparative evaluation of the potential of the above polymers as excipients for KT eyedrops. The drug–polymer interaction data obtained by NMR have been compared with data obtained by the dynamic dialysis, a time-honoured technique for determining drug–polymer binding, which basically consists in measuring the polymer effect on the drug permeation rate across a membrane permeable to the drug, impermeable to the polymer.[6]

2. Results and discussion

Ketotifen fumarate ^{1}H NMR spectrum in D_2O (pH 7.4) was characterized by combined 2D NMR experiments in order to assign aromatic protons which are not superimposed to polysaccharide resonances in the spectra of mixtures. Before starting the analysis of KT–polysaccharide interactions, we took into consideration KT self-aggregating propensity which, in principle, could have great relevance in heteroaggregation processes. To this aim we analysed ^{1}H NMR spectra of KT solutions, progressively diluted from 20 to 0.1 mM (Table 1).

In order to analyse chemical shifts dependence on concentrations gradients, Eq. 1, which expresses the observed chemical shift (δ_{obs}) as the average of the limit monomer (δ_M) and dimer (δ_D) chemical shifts, weighted for the respective molar fractions X_M and X_D, and Eq. 2, giving dependence of dimerization constant K_D on concentration C_0, were combined in the form of Eq. 3:

$$\delta_{obs} = X_M\delta_M + X_D\delta_D \quad (1)$$

$$K_D = \frac{X_D}{2C_0X_M^2} = \frac{X_D}{2C_0(1-X_D)^2} \quad (2)$$

$$C_0 = \frac{1}{2K_D}\frac{(\delta_{obs}-\delta_M)(\delta_D-\delta_M)}{(\delta_{obs}-\delta_D)^2} \quad (3)$$

Table 1
^{1}H NMR (600 MHz, D_2O, 25 °C) chemical shifts (δ, Hz) dependence of selected KT protons on concentration gradients

	δ (20 mM)–δ (0.1 mM)
H_1	−89.5
H_2	−83.1
H_3	−74.1
H_4	0

Eq. 3 was employed as a basis for experimental data fitting in order to extract self-association constant, which was equal to 0.1 M^{-1}, that is, very low. Therefore, at 2 mM concentration, which we considered in binding experiments, self-aggregation occurs to a very low extent and, thus, in the drug–macromolecule mixtures this process does not compete significantly with heteroaggregation phenomena.

The above conclusions were confirmed by NMR DOSY technique, which makes it possible to measure the translational diffusion coefficient D. This parameter depends on hydrodynamic radius (R_H) according to the Stokes–Einstein equation[4] (Eq. 4).

$$D = \frac{kT}{6\pi\eta R_H} \quad (4)$$

where k is the Boltzmann constant, η is the solvent viscosity, and T is the absolute temperature. Hence, D constitutes a size-dependent parameter. Thus, diffusion coefficient, which is a very sensitive probe of supramolecular aggregation processes, changed from 4.2×10^{-10} m^2 s^{-1} to 3.8×10^{-10} m^2 s^{-1} for pure KT at 2 mM and 10 mM, respectively, accordingly to fractions from 0.04% (2 mM) and 0.2% (10 mM). Interestingly, the counterion diffusion coefficient was remarkably higher ($D = 6.1 \times 10^{-10}$ m^2 s^{-1} at 2 mM and $D = 6.0 \times 10^{-10}$ m^2 s^{-1} at 10 mM) than that of KT, indicating a low degree of ion pairing.[7]

Selection of methods suited to investigate drug–macromolecule interactions essentially depends on the need to set a very high ligand:target ratio (from 20 to 100:1 or greater) in order to obtain a detectable NMR signal for the ligand. On the fast-exchange conditions and neglecting self-aggregation processes, the observed parameter represents the weighted average of its value in the bound and free states; thus only NMR parameters undergoing a sharp variation as the consequence of ligand–macromolecule interaction can be usefully exploited. Because binding-induced chemical shift changes are relatively small compared to the line width changes, most NMR studies have been focused on different NMR parameters such as relaxation rates,[3,8] or magnetization transfer techniques.[9]

In particular it has been shown that the selective relaxation rate (R) of the ligand is a more sensitive indicator of binding than non-selective rate (R^{ns}) is. In fact, methods based on the determination of the selective relaxation rates take advantage of the favourable dependence of R on the correlation time in the region of slow molecular motions, in which the small molecule is forced by the interaction with the macromolecule. In the fast-motion region ($\omega^2\tau_c^2 \ll 1$; ω = Larmor frequency, τ_c = reorientational correlation time), both the selective (R) and non-selective (R^{ns}) relaxation rates increase progressively with increasing τ_c.[3] When the molecular motion of the ligand is slowed down to the $\omega^2\tau_c^2 \gg 1$ region as a consequence of the interaction with the macromolecule, R shows a sharp increase, whereas R^{ns} reaches a maximum for $\omega^2\tau_c^2 \cong 1$ and then decreases with further increasing $\omega^2\tau_c^2$. In the presence of well-resolved proton resonances, selective relaxation rates can be easily determined by selective excitation of only one spin, leaving other ones unperturbed, and following the magnetization recovery in the time. In the fast-exchange limit, the measured relaxation rates (R_{obs}) are the weighted means of the values in the bound (R_b) and free (R_f) states (Eq. 5).

$$R_{obs} = X_bR_b + X_fR_f \quad (5)$$

where X_b and X_f are the molar fractions of the bound and free conditions. As the concentration of the ligand is much higher than that of the polymer, then $X_f \cong 1$, and

$$R_{obs} = X_bR_b + R_f \quad (6)$$

For the 1 to 1 complexation macromolecule (M)/ligand (L) equilibrium, where [L] ≫ [M], Eq. 6 can be expressed as follows[2]:

$$R_{obs} = \frac{KR_b[M_0]}{1 + K[L]} + R_f \quad (7)$$

where K is the heteroassociation constant and $[M_0]$ is the initial macromolecule concentration. The plot of R_{obs} versus $[M_0]$ should give a straight line, the slope of which is defined as 'affinity index' ([A]), a parameter which depends on the temperature and ligand concentration (Eq. 8).

$$[A] = \frac{KR_b}{1 + K[L]} \quad (8)$$

In case of n binding sites of equal strength, the affinity index takes different forms,[10] but in any situation, the relationship between R_{obs} and $[M_0]$ is always linear (Eq. 9) and thus the parameter [A] is independent of the complexation stoichiometry and constitutes a powerful tool for comparing the ligand–macromolecule affinities.

$$R_{obs} = R_f + [A][M_0] \quad (9)$$

Different sites of the molecule can have different affinity indexes, which must be normalized on the basis of the respective selective relaxation rates in the free states (R_f). Thus a normalized affinity index[11] $[A^N]$ can be obtained (Eq. 10), which provides a measure of ligand–macromolecule global affinity.

$$[A^N] = \frac{[A]}{R_f} \quad (10)$$

Further information on the drug–macromolecule interaction can also be obtained by determining the cross-relaxation term σ_{ij},[12] which describes the magnetization transfer between the proton pair ij. σ_{ij} is a function of the reorientational correlation time τ_c of the vector connecting the two spins i and j and of their distance r_{ij} (Eq. 11):

$$\sigma_{ij} = f\left(r_{ij}^{-6}, \tau_c\right) \quad (11)$$

The cross-relaxation parameters can be determined in a very simple way by measuring the proton mono- (R) and biselective (R^{bs}) relaxation rates,[3] which are determined by inverting simultaneously the proton pair ij and following the recovery of i in time. On subtracting R_{ij}^{bs} from R_i, the cross-relaxation rate σ_{ij} can be calculated (Eq. 12), and, hence, the σ_{ij} values for proton pairs at fixed distances can be usefully correlated to the reorientational correlation time, which is a parameter very sensitive to the drug–macromolecule interaction.[3,13] In particular, in the slow-motion region, which is typical of macromolecule bound ligands, negative σ_{ij} values are obtained and, hence, a decrease of σ_{ij} with respect to the free value must be expected, the extent of which depends on the bound molar fraction.

$$\sigma_{ij} = R_{ij}^{bs} - R_i \quad (12)$$

First of all we measured proton selective relaxation rates of KT at 2 mM concentration in D_2O (pH 7.4, phosphate buffer) and compared free state values to those measured in the presence of each polysaccharide (4 mg/mL, D_2O, pH 7.4).

As an example, for pure KT the selective relaxation rate of aromatic proton named H_2 was 0.56 s^{-1} (Table 2), which in the presence of TSP increased to 0.89 s^{-1}. As a consequence of the interaction between the drug and the polysaccharide, smaller variations of the relaxation rate of the same proton were detected in the mixture containing HEC (0.62 s^{-1}), as reported in Table 2. An even smaller variation to 0.58 s^{-1} was measured in the case of HA. Proton H_1 belonging to the same sulfurate aromatic ring changed its relaxation parameter from 0.26 s^{-1}, in the pure compound, to 0.49 s^{-1} in the presence of TSP, whereas only smaller or no increases were detected in the presence of HEC and HA, that is, to 0.30 and 0.26 s^{-1}, respectively (Table 2). The same trend was also observed for KT proton H_3 of the phenyl ring (Table 2). Unfortunately selective relaxation rate of protons H_4, H_5 and H_6 could not be measured due to the extensive superimposition of their resonances.

Table 2
Selected ^1H (600 MHz, D_2O, 25 °C) selective relaxation rates (s^{-1}) of KT (2 mM), and its mixtures with polysaccharides, TSP, HA or HEC (4 mg/mL)

	H_1	H_2	H_3	H_{13}
KT	0.26	0.56	0.38	0.09
KT/TSP	0.49	0.89	0.86	0.08
KT/HEC	0.30	0.62	0.48	0.08
KT/HA	0.26	0.58	0.48	0.07

Fumarate counterion proton selective relaxation rates underwent small but reproducible decreases in the three mixtures (Table 2) to indicate that it is involved in the ligand–macromolecule interaction to a very low extent. Interestingly, a negligible dependence of counterion relaxation parameter on polymer concentration even at the highest macromolecule concentration (8 mg/mL) allowed us to conclude that the variations detected for the KT parameter cannot be ascribed to viscosity changes.

In order to compare binding processes, the [A] values for KT and the three polysaccharides were calculated from the slope of the line describing the dependence of proton selective relaxation rates on macromolecule concentration. To this aim we calculated proton selective relaxation rates of 2 mM KT in the presence of different concentrations of each polymer progressively increasing from 0.5 to 8 mg/mL.

Corresponding data are shown for proton H_1, H_2 and H_{13} in the Figures 2–4. On the basis of linear fitting of data (Figs. 2–4), affinity indexes for the different KT protons were calculated as reported in Table 3.

The above data were further normalized with respect to R_f in order to obtain normalized affinity indexes $[A^N]$ (Table 3).

These were remarkably higher in the presence of TSP, whereas significantly lower values were calculated in the presence of the other two polymers. In particular, HA seemed to be the polymer with the lowest binding affinity among the three polysaccharides. It is noteworthy that also the stability of the three kinds of mix-

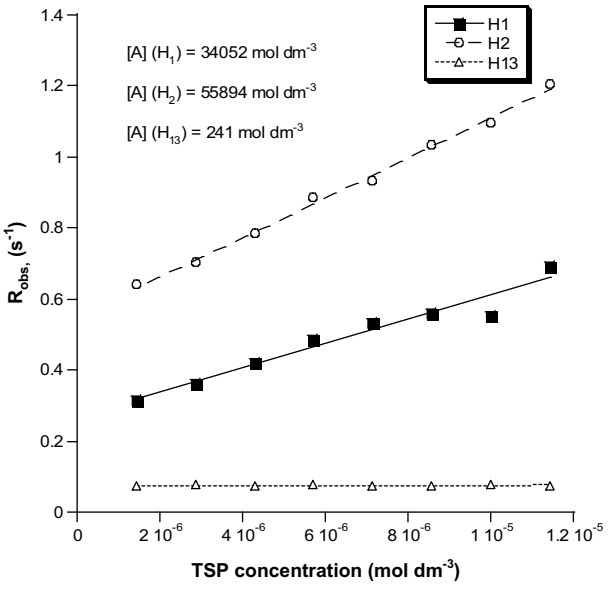

Figure 2. Dependence of selective relaxation rates (R_{obs}, s^{-1}) on TSP concentration (mol dm^{-3}).

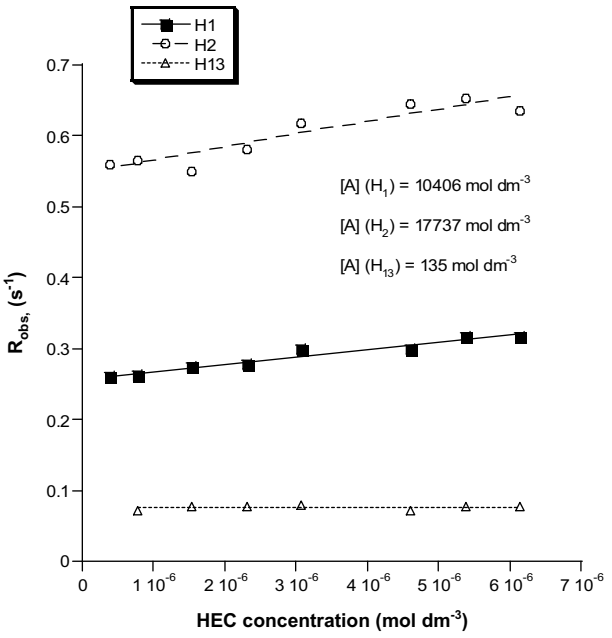

Figure 3. Dependence of selective relaxation rates (R_{obs}, s^{-1}) on HEC concentration (mol dm^{-3}).

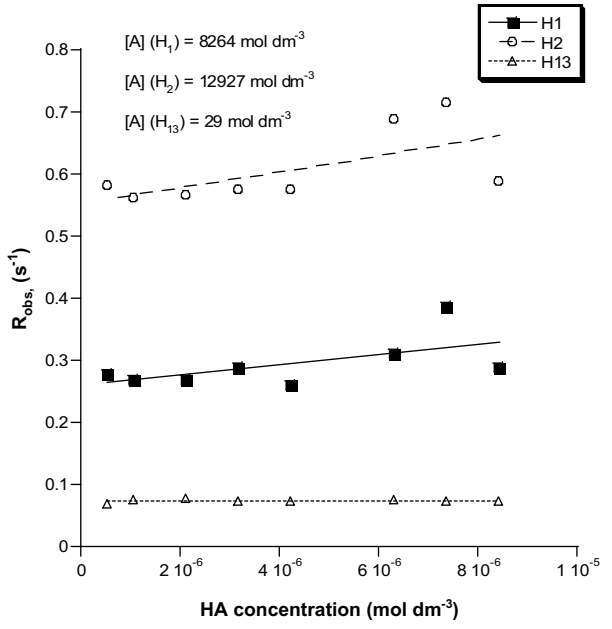

Figure 4. Dependence of selective relaxation rates (R_{obs}, s^{-1}) on HA concentration (mol dm^{-3}).

Table 3
Affinity indexes ([A], $dm^3\ mol^{-1}\ s^{-1}$) and normalized affinity indexes ([A^N], $dm^3\ mol^{-1}$) calculated for selected protons of KT (2 mM) with TSP, HA or HEC

	H_1		H_2		H_3	
	[A]	[A^N]	[A]	[A^N]	[A]	[A^N]
KT/TSP	34,052	130,467	55,894	99,279	71,267	149,094
KT/HEC	10,406	39,870	17,737	31,504	44,619	93,345
KT/HA	8264	31,785	12,927	23,084	25,777	53,702

tures was checked in time, by repeating proton selective relaxation rate measurements after 3 and 5 weeks. Relaxation parameters of KT in mixture with TSP or HEC remained unchanged with respect to values measured immediately after their preparation, whereas in the mixture KT-HA precipitation of drug occurred, as clearly demonstrated by the fact that in the ^1H NMR spectrum a remarkable change of relative integrated areas of KT and counterion protons were detected (Fig. 5).

Interestingly, differences in the normalized affinity index of the three protons H_1, H_2 and H_3 in each mixture can be helpful to identificate drug sites more extensively involved in the interaction with the macromolecule. Thus, for TSP an extensive involvement of also the sulfurate moiety can be pointed out, which is less significant in the interaction of KT with HA or HEC.

Finally, we calculated, for pure KT (2 mM) and for its mixtures with each of the three biopolymers (4 mg/mL), the cross-relaxation rate of the proton pair H_1–H_2. To this aim, we measured the bisselective relaxation rates of proton H_2 on simultaneous inversion of proton H_1 on the same aromatic ring: the value of 0.60 s^{-1} was obtained for pure KT, whereas in the presence of TSP, HEC, or HA the values of 0.86 s^{-1}, 0.65 s^{-1} or 0.61 s^{-1} were obtained. By using Eq. 12, the cross-relaxation term of 0.04 s^{-1} was calculated for pure KT, and in the three mixtures the values of 0.03 s^{-1} (HA), 0.03 s^{-1} (HEC) and −0.03 s^{-1} (TSP) were obtained (Table 4). The above values are in accordance with the higher KT affinity for TSP. In fact, in the TSP-containing mixture the ligand experienced slow motions in which it was forced as a consequence of the interaction with the macromolecule. This brought about the negative value of σ_{12} which is characteristic of the macromolecule. In the other two cases (HEC and HA), the small variation of the cross-relaxation terms in comparison to the pure drug reflected the smaller molar fractions bound to polymer and hence the smaller ability of the two polysaccharides to interact with KT.

KT binding to TSP, HA or HEC was also studied by a technique quite different from NMR, that is, the dynamic dialysis, and the results obtained by the two techniques were compared to verify their agreement, and hence, their validity. The polymer effect on the drug permeation rate across a porous membrane was determined. The molecular weight cutoff of the membrane, 3500 Da, was well above the molecular size of KT and much below that of whichever polymer, so the membrane was permeable by the free drug but impermeable to the polymers and the drug–polymer complexes. If the drug trans-membrane flux is supposed to occur by passive diffusion, under quasi-steady state conditions, and if sink conditions are assumed (drug concentration in receptor medium negligible with respect to that in donor medium), then the dialysis of the drug in the absence of polymer (control) is expected to follow 1st order kinetics, described by the following equations:

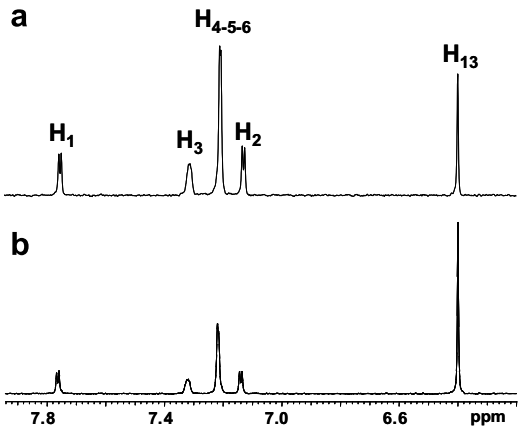

Figure 5. High-frequency ^1H NMR (600 MHz, D_2O, pH 7.4, 25 °C) spectral region of the mixture KT/HA (2 mM KT, 4 mg/mL HA) immediately after mixture dissolution (a) and after 3 weeks from the preparation of the mixture (b).

Table 4
Cross relaxation rates (σ_{12}, s^{-1}, 25 °C, D_2O, 600 MHz) of KT (2 mM), and its mixtures with polysaccharides, TSP, HA or HEC, (4 mg/mL)

	σ_{12}
KT	0.04
KT/TSP	−0.03
KT/HA	0.03
KT/HEC	0.03

$$\frac{dC}{dt} = -K_c C \quad (13)$$

$$\ln C = \ln C_0 - K_c t \quad (14)$$

where C_0 and C represent the drug concentration in the donor at time zero and t, respectively, and K_c is the dialysis rate constant for the control. In fact, when Eq. 14 was fitted by linear regression to dynamic dialysis data for KT in the absence of polymers, presented in Figure 6, a high r^2 value resulted (0.997). When a polymer interacting with the drug, such as TSP, HA or HEC, is added to the donor solution, the dialysis rate should be proportional to the concentration of free, non-interacting drug, according to the following equation:

$$\frac{dC}{dt} = -K_c(1 - f_b)C \quad (15)$$

where f_b is the drug fraction bound to the polymer. In fact, when $\ln C$ was plotted versus time highly significant straight lines were obtained (r^2 values, 0.998, 0.999, and 0.999, with TSP, HA and HEC, respectively), as appears in Figure 6.

Each line is described by the following equation, obtained by integration of Eq. 15 under the assumption that f_b is constant in the C range of the dynamic dialysis experiment:

$$\ln C = \ln C_0 - K_c(1 - f_b)t \quad (16)$$

Thus, the f_b value for each polymer could be calculated from the ratio between the slope of the relative straight line, $S_p = K_c(1 - f_b)$, and that of the control, K_c

$$f_b = 1 - \frac{S_p}{K_c} \quad (17)$$

The obtained values of K_c, S_p and f_b at 25 °C are listed in Table 5. As can be seen, the f_b values are in the rank order KT/TSP>KT/HEC>KT/HA, in line with the rank order of the affinity indexes and normalized affinity indexes listed in Table 5.

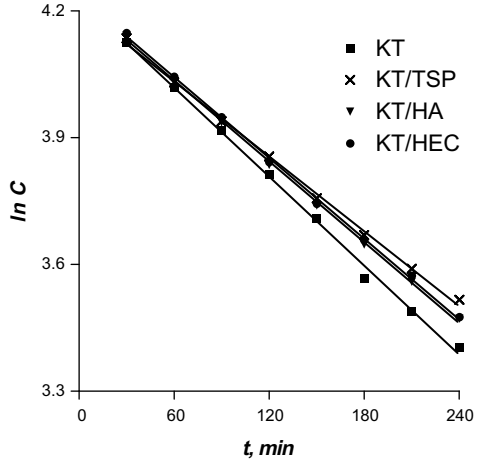

Figure 6. Plots of dynamic dialysis data according to Eq. 16.

Table 5
Dynamic dialysis data

	$K_c \times 10^3$ min^{-1}	$S_p \times 10^3$ min^{-1}	f_b	r^2
KT	3.512±0.078	—	—	0.997
KT/TSP	—	2.956±0.053	0.16	0.998
KT/HA	—	3.194±0.044	0.09	0.999
KT/HEC	—	3.188±0.044	0.09	0.999

The drug and polymer concentrations in the donor, that is, 0.7 mg/mL and 0.2%, respectively, were chosen as suitable for therapeutic eyedrops.

3. Conclusion

In spite of high structural complexity of drug formulations involving polysaccharides as controlled release systems, which, in principle, makes spectroscopic investigations a challenging effort, NMR spectroscopy fully confirms its versatility and efficiency also in this field. Several fundamental aspects can be accurately ascertained by detecting NMR parameters, such as selective relaxation rates and diffusion coefficients, which are very sensitive probe of drug–drug and drug–polysaccharide interactions.

In this way ketotifen–polysaccharide systems were investigated, which constitutes the basis of already proposed formulations for ophthalmic uses. Remarkably higher KT affinity for TSP than for HEC or HA was clearly demonstrated. In agreement with these results, the KT fraction bound to TSP, as determined by the dynamic dialysis technique, was significantly higher than that bound to HEC or HA. On the basis of NMR investigations, the comparatively enhanced affinity of KT for TSP can reasonably be attributed to an ability of this polymer to originate extensive interactions with the drug. Such interactions, also involving the KT sulfurate moiety, were probably determined by expected significant differences in secondary structure between TSP and the other polymers. Regarding the stability of the drug–polysaccharide mixtures, which could have great relevance to the properties of their medical formulations, another fundamental aspect was demonstrated, that is, both TSP and HEC form stable mixtures with KT, whereas in the presence of HA drug precipitation occurs in time.

Above findings strongly suggest great relevance of TSP in the development of new controlled drug release formulations, also taking into account its already proved[5a,b] mucoadhesive properties.

4. Experimental

4.1. General methods

NMR measurements were performed on spectrometer operating at 600 MHz for ^1H. The temperature was controlled to 25±0.1 °C. The 2D NMR spectra were obtained by using standard sequences. Proton gCOSY 2D spectrum, which was employed for the characterization, was recorded in the absolute mode acquiring 4 scans with a 10 s relaxation delay between acquisitions for each of 256 FIDs. The selective relaxation rates were measured in the initial rate approximation by employing a selective π-pulse at the selected frequency. After the delay τ, a non-selective π/2 pulse was employed to detect the longitudinal magnetization.

DOSY experiments were carried out by using a stimulated echo sequence with self-compensating gradient schemes, a spectral width of 8000 Hz and 64 K data points. A value 180 ms was used for Δ, 1.0 ms for δ, and g was varied in 30 steps (16 transients each) to obtain an approximately 90–95% decrease in the resonance intensity at the largest gradient amplitudes. The baselines of all arrayed spectra were corrected prior to processing the data. After data acquisition, each FID was apodized with 1.0 Hz line

broadening and Fourier transformed. The data were processed with the DOSY macro (involving the determination of the resonance heights of all the signals above a pre-established threshold and the fitting of the decay curve for each resonance to a Gaussian function) to obtain pseudo two-dimensional spectra with NMR chemical shifts along one axis and calculated diffusion coefficients along the other.

The solutions for the NMR experiments were obtained by mixing different volumes of stock solutions of the appropriate amounts of ligand and polysaccharides. In the binding experiments ketotifen concentration was 2 mM.

For determining KT–polymer interaction by the dynamic dialysis technique a diffusion cell, apparatus and procedure similar to those described by Bottari et al.[6] were used. KT flux through a porous cellulose membrane (Spectra/Por®, molecular weight cutoff, 3500 Da, Spectrum Laboratories Inc., Rancho Dominguez, CA, USA) was measured at 25 °C under conditions of validity of Eqs. 13 and 14. The initial concentration of the stirred KT solution in phosphate buffer 0.0375 M, pH 7.4 at the donor side of membrane was 0.7 mg/mL, lower than solubility. Sink conditions were ensured at the receptor side of the membrane, that is, the drug concentration in receptor medium (5 mL) was negligible with respect to that in donor medium (100 mL). At measured time intervals the KT concentration in the receiving phase was spectrophotometrically determined, at 301 nm, to calculate the cumulative amount permeated in time t, from which the drug concentration in donor medium at time t could be calculated.

4.2. Materials

Ketotifen fumarate, hydroxyethylcellulos (1300 kDa), hyaluronic acid (950 kDa) and the polysaccharide extracted from tamarind seeds (700 kDa) were provided by Farmigea SpA (Pisa, Italy).

Acknowledgment

The work was supported by MIUR (FIRB Project RBPR05NWWC).

References and notes

1. (a) Shapiro, M. J. *Am. Pharm. Rev.* **2002**, *5*, 94; (b) Fielding, L. *Prog. Nucl. Magn. Reson. Spectrosc.* **2007**, *51*, 219.
2. Rossi, C.; Donati, A.; Bonechi, C.; Corbini, G.; Rappuoli, R.; Dreassi, E.; Corti, P. *Chem. Phys. Lett.* **1997**, *264*, 205.
3. Valensin, G.; Sabatini, G.; Tiezzi, E. In *Advanced Magnetic Resonance Techniques in Systems of High Molecular Complexity*; Niccolai, N., Valensin, G., Eds.; Birkhauser: Boston, 1986; pp 69–76.
4. Johnson, C. S., Jr. *Prog. Nucl. Magn. Reson. Spectrosc.* **1999**, *34*, 203.
5. (a) Burgalassi, S.; Raimondi, L.; Pirisino, R.; Banchelli, G.; Boldrini, E.; Saettone, M. F. *Eur. J. Ophthalmol.* **2000**, *10*, 71; (b) Rolando, M.; Valente, C. *BMC Ophthalmol.* **2007**, *7*, 5; (c) Gidley, M. J.; Lillford, P. J.; Rowlands, D. W.; Lang, P.; Dentini, M.; Crescenzi, V.; Edwards, M.; Fanutti, C.; Grant Reid, J. S. *Carbohydr. Res.* **1991**, *214*, 299.
6. Bottari, F.; Di Colo, G.; Nannipieri, E.; Saettone, M. F.; Serafini, M. F. *J. Pharm. Sci.* **1975**, *64*, 946.
7. Pregosin, P. S. *Prog. Nucl. Magn. Reson. Spectrosc.* **2006**, *49*, 261.
8. Valensin, G.; Kushnir, T.; Navon, G. *J. Magn. Reson.* **1982**, *46*, 23.
9. (a) Klein, J.; Meinecke, R.; Mayer, M.; Meyer, B. *J. Am. Chem. Soc.* **1999**, *121*, 5336; (b) Dalvit, C.; Pevarello, P.; Tato, M.; Veronesi, M.; Vulpetti, A.; Sundstrom, M. *J. Biomol. NMR* **2000**, *18*, 65; (c) Meyer, B.; Peters, T. *Angew. Chem., Int. Ed.* **2003**, *42*, 864.
10. Rossi, C.; Bastianoni, S.; Bonechi, C.; Corbini, G.; Corti, P.; Donati, A. *Chem. Phys. Lett.* **1999**, *310*, 495.
11. Corbini, G.; Martini, S.; Bonechi, C.; Casolaro, M.; Corti, P.; Rossi, C. *J. Pharm. Biomed. Anal.* **2006**, *40*, 113.
12. Neuhaus, D.; Williamson, M. *The Nuclear Overhauser Effect in Structural and Conformational Analysis*; VCH Publisher: New York, 1989.
13. Uccello-Barretta, G.; Bertucci, C.; Domenici, E.; Salvadori, P. *J. Am. Chem. Soc.* **1991**, *113*, 7017.